Morphology, ^{31}P Spin Diffusion, and Phase Transitions in a Representative Semicrystalline Polyphosphazene by Solid-State NMR

Sharon A. Taylor, Jeffery L. White, Nick C. Elbaum, Richard C. Crosby,‡ Gordon C. Campbell,† and James F. Haw*

Department of Chemistry, Texas A&M University, College Station, Texas 77843

Galen R. Hatfield

W. R. Grace and Company, Washington Research Center, 7379 Route 32, Columbia, Maryland 21044

Received July 17, 1991; Revised Manuscript Received January 28, 1992

ABSTRACT: Solid-state NMR spectroscopy was used to investigate the morphology and molecular dynamics of poly[bis(3-methylphenoxy)phosphazene] (PB3MP), a representative semicrystalline polyphosphazene. Variable-temperature ^{31}P magic-angle spinning (MAS) NMR spectra revealed two well resolved isotropic resonances for the crystalline and mesomorphic phases. The ability to resolve resonances for the two phases makes this class of polymers well suited for studying morphology and phase transitions using NMR. ^{31}P spin–lattice relaxation (T_1) behavior for PB3MP at 23 °C suggested that spin diffusion occurs between the two phases, which was confirmed by the observation of cross peaks in a two-dimensional exchange experiment. The measured ^{31}P spin diffusion rate is intermediate between the well-established limits of ^{1}H and ^{13}C spin diffusion, and its appears as an apparent anomaly in the ^{31}P spin–lattice relaxation behavior. Employing a model diffusion equation, the spin diffusion rate constant was used to estimate a characteristic diffusion distance of 4.5 nm, implying a lamellar thickness of ca. 9 nm. The amplitude of side-group motion in the crystalline and mesomorphic phases was investigated by the analysis of sideband patterns in ^{13}C MAS spectra obtained at slow spinning speeds. Negligible motion occurs in the crystalline phase, whereas large amplitude motion occurs in the mesomorphic phase. Variable-temperature ^{31}P and ^{1}H rotating frame spin–lattice relaxation ($T_{1\rho}$) studies revealed activation energies of ca. 10 kcal/mol for motion in the mesomorphic phase.

Introduction

Phase separation into supramolecular entities of differing composition, mobility, and size is a key determinant of mechanical, optical, and other properties of solid polymers. Although phase separation is often apparent in thermal or diffraction measurements, the detailed characterization of phase-separated polymers requires spectroscopic techniques that can both probe specific functional groups or atomic sites and differentiate between the various phases. NMR spectroscopy has long been applied to this task with atomic site differentiation achieved through isotropic chemical shift (e.g. ^{13}C) or selective labeling (e.g. ^{2}H) and phase recognition based primarily upon the effects of molecular motion on spectroscopic observables such as relaxation rates or line widths. Less commonly, phase differentiation can be obtained based on isotropic chemical shift differences,[1-3] which in turn reflect differences in static or time-averaged conformations or packing effects. The theoretical basis necessary to relate line shapes and relaxation rates to the amplitudes and frequencies of molecular motion was worked out early in the history of NMR,[4] and a large number of studies have probed dynamics in both homogeneous and phase-separated polymers.[5-12]

In some phase-separated polymers, supramolecular structures such as spherulites are large enough to be detected and measured by microscopy. In many semicrystalline polymers, however, the crystallites are too small to be resolved in SEM photographs, and less direct methods are necessary in order to measure a characteristic size. One such method makes use of the NMR phenomenon of spin diffusion,[13] which involves megnetization transfer over a distance through a series of discrete spin–spin flip–flops.[14] The rates of these zero-quantum transitions scale as the inverse sixth power of the internuclear separation and the fourth power of the magnetogyric ratio, γ. For protons in most polymers (or ^{19}F in fluoropolymers) the concentration of spins is sufficiently high that the propagation of magnetization between spatial regions separated by several nanometers or more can be accurately modeled as a diffusional process.[15] Indeed, proton spin diffusion in typical organic solids propagates magnetization over a distance that increases as $t^{1/2}$, as is typical of a diffusional process. For rare spins such as ^{13}C, however, it may not be appropriate to model the propagation of magnetization through space as a diffusional process, and natural abundance ^{13}C "spin-diffusion" measurements in organic solids have proven difficult to quantify in terms of a distance versus time dependence.[16]

In spite of the many applications of NMR to the characterization of polymer morphology, there has been little effort thus far to use sophisticated NMR methods in a variable-temperature mode to understand the details of phase transitions in polymers.[17-19] In the course of studying the morphologies of a variety of semicrystalline polyphosphazenes,[20] we have noted several properties which make them well suited for an exploration of polymer phase transitions by NMR. At moderate magnetic field strengths (≥7 T), many semicrystalline polyphosphazenes have well-resolved ^{31}P isotropic chemical shifts corresponding to the crystalline and mesomorphic phases. This contrasts with the typical case in ^{13}C spectroscopy in which fully resolved resonances reflecting phase separation are

* Author to whom correspondence should be addressed.
† Present address: Central Research and Development, Experimental Station, E. I. Dupont de Nemours and Company, Wilmington, DE 19898-0328.
‡ Present address: GE Plastics, 1 Lexan Lane, Mt. Vernon, IN 47620.

0024-9297/92/2225-3369$03.00/0

less common. Easily resolved spectral features due to the two phases facilitate the independent measurement of various relaxation rates in the two phases over a range of temperatures. Finally, the presence of ^{31}P at a concentration of one nucleus per repeat unit creates the possibility for spin diffusion phenomena in a regime intermediate between the cases for ^{1}H and ^{13}C at natural abundance.

We report here a detailed study of the above phenomena for the specific case of poly[bis(3-methylphenoxy)phosphazene] (PB3MP). Preliminary results with other semi-

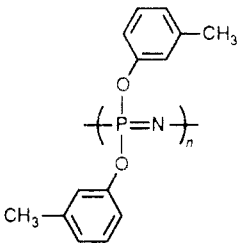

PB3MP

crystalline polyorganophosphazenes suggests that the properties of PB3MP are representative. Our NMR results are in accord with the well-established view that the transition to mesomorphic phase permits large amplitude (but not isotropic) motion.[21-23]

A dominant feature of many of the ^{31}P experiments was ^{31}P spin diffusion between the two phases with a temperature-independent rate constant of ca. 0.3 s^{-1}. Drawing from some of VanderHart's work on proton spin diffusion in polymers,[15] we use this measurement to estimate a lamellar thickness of ca. 9 nm. The intermediate rate of spin diffusion observed in these studies is particularly easy to recognize and interpret, and it will be interesting to see if similar effects can be observed in other phosphorus-containing polymers or samples enriched in ^{13}C.

Experimental Section

Reagents. Poly[bis(3-methylphenoxy)phosphazene] (PB3MP) was provided by the Shin Nisso Kako Co., Ltd., of Japan. A sample of PB3MP synthesized in our laboratory displayed the same NMR properties as the commercial sample reported in this paper. All results reported here were obtained for the commercial sample.

Polymer Characterization. The semicrystalline nature of this polymer was confirmed by X-ray diffraction analysis using a Philips APD 3720 diffractometer and Cu irradiation. The data were obtained using a 0.020° step size over 4–80° (2θ range) and 0.5 s count time. The liquid crystalline nature of this polymer was confirmed by hot-stage polarized light microscopy. The micrograph exhibited large regions of birefringence on the order of 0.2 mm.

Samples for scanning electron microscopy were mounted onto SEM stubs using conductive carbon paint and then coated with a thin film of gold to ensure a good conductive surface for the electron beam. Secondary electron images were then obtained on a Hitachi 570 SEM using a beam accelerating voltage of 5.0 kV. No spherulites or other structures larger than the resolution limit of the images (3 μm) were observed for samples identical to those studied by NMR.

Differential scanning calorimetry was performed using two instruments, a Perkin-Elmer DSC II equipped with a subambient accessory, and a Perkin-Elmer Series 7 instrument with associated robotics. Subambient scans confirmed the glass transition at −25 °C. When rapid (i.e. ≥10 °C/min) scans were made in the heating direction, a sharp peak corresponding to the mesomorphic transition was observed at ca. 78 °C. Upon rapid cooling, this transition was observed at ca. 63 °C. At slower heating or cooling rates, the DSC peak broadened severely, suggesting that the transition in fact occurs over a broad temperature range. This observation is consistent with the picture revealed by the NMR experiments (vide infra).

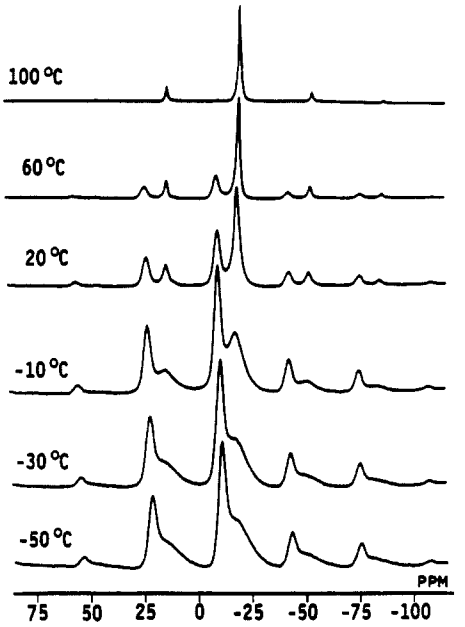

Figure 1. Variable-temperature ^{31}P MAS Bloch decay spectra of PB3MP showing isotropic peaks at −10.7 ppm (crystalline) and −19.4 ppm (mesomorphic) and their associated spinning sidebands.

NMR Measurements. Magic-angle spinning (MAS) NMR spectra were acquired using a Chemagnetics CMX-300 NMR spectrometer operating at 121.3 MHz (^{31}P) and 75.3 MHz (^{13}C). Typical spectra were recorded using a 30-kHz spectral width, an acquisition length of 1K data points, and 25 Hz (^{31}P) or 50 Hz (^{13}C) of line broadening. A 90° pulse width of 4.3–4.5 μs was used. In cross polarization experiments, a 58-kHz spin-lock field and a contact time of 4 ms were used unless otherwise noted. All spectra were externally referenced to hexamethylbenzene (HMB) (^{13}C, aliphatic peak at 17.4 ppm) and 2(*S*),3(*S*)-(−)-bis(diphenylphosphino)butane (Chiraphos) (^{31}P, −14.10 ppm); both standards were obtained from Aldrich. ^{31}P two-dimensional exchange spectra were obtained using standard methods.[24,25] The number of data points accumulated in the t_1 and t_2 time domains were 128 and 256, respectively, with subsequent zero-filling in the t_2 dimension. Two-dimensional spectra were acquired at mixing times ranging from 0 to 4 s.

To accurately characterize the magnetization decay in relaxation measurements, spectra were acquired at 12–14 τ values ranging from 0 to $>5T_1$ for T_1 measurements and from 0 to 16 ms for $T_{1\rho}$ measurements. T_1 values for ^{31}P were obtained using the method developed by Torchia,[26] while ^{1}H T_1 values were measured using the method described by Maciel et al.[27]

Results and Discussion

The temperature-dependent morphology of PB3MP is readily apparent in the ^{31}P MAS NMR spectra in Figure 1. These spectra reveal the isotropic resonances at −19.4 and −10.7 ppm. The −10.7 ppm peak sharpens slightly at temperatures above ca. −30 °C (in the vicinity of T_g). As the sample was heated from −50 °C to 100 °C, the −19.4 ppm resonance grew at the expense of that at −10.7 ppm. At low temperatures, the −19.4 ppm peak broadened. This broadening is attributed to a dispersion of isotropic chemical shifts due to conformational differences. The presence of spinning sidebands for the −19.4 ppm peak at 100 °C indicates that appreciable chemical shift anisotropy remains above the mesomorphic phase transition. The motion at this temperature is highly anisotropic because of constraints associated with the liquid crystalline nature of this polymer.

All of our variable-temperature NMR studies were performed with temperature changes of less than 5 °C/

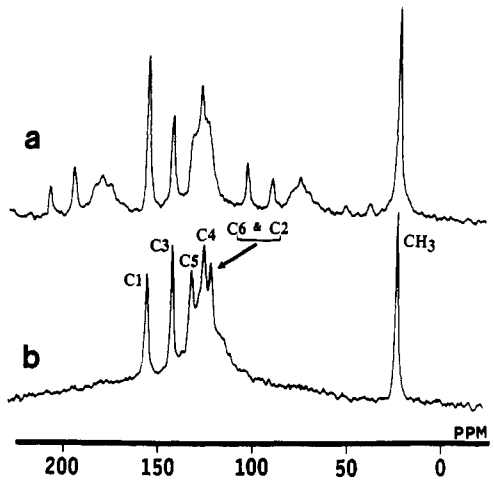

Figure 2. ^{13}C MAS NMR spectra of PB3MP using (a) cross polarization to emphasize the crytalline phase and (b) a 90° pulse (Bloch decay) with a 20-s pulse delay to emphasize the mesomorphic phase. Assignments were made by analogy to *m*-cresol.

min and equilibration times of at least 5 min. With this protocol, reproducible results were obtained in both the heating and cooling direction. No hysteresis was observed using the above protocol for PB3MP, although we have observed such effects in NMR studies of other polyphosphazenes.[28] We assigned the resonance at −19.4 ppm to the mesomorphic phase (which is favored at higher temperatures) and that at −10.7 ppm to the crystalline phase. Further support for these assignments were obtained from relaxation measurements (vide infra) as well as the observation that the ^{31}P spectrum of PB3MP in solution has a single resonance at −19.4 ppm.

Resolution of the crystalline and mesomorphic phases on the basis of ^{13}C isotropic chemical shifts was not observed, but it was possible to selectively observe ^{13}C magnetization for either phase by a suitable choice of excitation conditions. Figure 2 illustrates this for PB3MP at 23 °C: the cross polarization spectrum (Figure 2a) emphasizes the prominent spinning sidebands expected for a slow-speed MAS spectrum of a rigid solid, whereas the Bloch decay spectrum (Figure 2b) obtained with a relatively short pulse delay discriminates in favor of mobile components and hence shows no sidebands. Thus, it was possible to independently measure ^{13}C relaxation behavior for the two phases based on choice of excitation, and/or by fitting selected portions of relaxation plots showing biexponential behavior. The ^{13}C NMR signals are from nuclei in the side groups. The absence of spinning sidebands in the ^{13}C NMR spectrum of the mesomorphic phase indicates that side group motion is more isotropic than backbone motion.

Table I reports ^{31}P and ^{1}H rotating frame relaxation times ($T_{1\rho}$) for the two phases over a range of temperatures. The ^{31}P $T_{1\rho}$ values for the crystalline phase were on the order of 100 ms and were not measured more accurately. Table II reports ^{13}C $T_{1\rho}$ values for the mesomorphic phase only. Schaefer has previously shown that spin–spin contributions to long $T_{1\rho}$ values invalidate their use in characterizing molecular dynamics.[29] All ^{1}H relaxation times were measured indirectly through cross polarization to the resolved ^{31}P signals. ^{1}H and ^{31}P spin–lattice relaxation times in the laboratory frame (T_1) as a function of temperature are reported in Table III. Detailed ^{13}C T_1 measurements were not attempted, but as was noted previously, there were large differences between the T_1s in the crystalline and mesomorphic phases which could be exploited to obtain a Bloch decay spectrum of pure mesomorphic phase by using a pulse delay of several seconds or less.

Table I
^{1}H and ^{31}P $T_{1\rho}$ Values for PB3MP

temp (°C)	^{1}H $T_{1\rho}$ (ms) crystalline	^{1}H $T_{1\rho}$ (ms) mesomorphic	^{31}P $T_{1\rho}$ (ms) mesomorphic[a]
−50	47.6	12.3	71.4
−30	43.5	8.5	27.8
−20	40.0	8.7	27.8
−10	33.3	1.4	20.0
0	33.3	4.3	11.2
10	31.3	2.6	13.5
23	16.7	2.9	5.2
40	19.2	6.9	8.5
60	15.9	20.8	23.2
80	12.4	47.6	47.6

[a] The corresponding ^{31}P $T_{1\rho}$ values for the crystalline phase were ≥100 ms and were not measured more accurately.

Table II
^{13}C $T_{1\rho}$ Values (ms) for the Mesomorphic Phase of PB3MP

temp (°C)	CH_3	C3 and C6	C4	C5	C3	C1
23	14.1	1.8	1.6	1.6	7.0	7.5
40	27.0	7.5	7.2	8.2	20.0	17.9
60	45.5	18.2	14.3	13.3	32.3	35.7
80	66.7	22.2	20.8	23.3	62.5	50.0

Table III
^{1}H and ^{31}P T_1 Values for PB3MP

temp (°C)	^{1}H T_1 (s) crystalline	^{1}H T_1 (s) mesomorphic	^{31}P T_1 (s) crystalline	^{31}P T_1 (s) mesomorphic
23	2.4	2.4	19.2	22.2
40	1.8	1.7	20.0	18.2
60	1.7	1.4	18.2	13.3
80	1.2	1.1	15.2	11.5

Detailed relaxation data such as those in Tables I–III can frequently be interpreted in terms of molecular dynamics, and we will return to some of these data for that purpose later in this contribution. For now, however, we wish to note several semiquantitative features of the relaxation data. Considering these data, one notes that the ^{1}H T_1 and ^{31}P T_1 values are each identical for the two phases, whereas the two phases displayed different ^{1}H $T_{1\rho}$, ^{31}P $T_{1\rho}$, ^{13}C $T_{1\rho}$, and ^{13}C T_1 values. In homogeneous solids, spin diffusion between abundant nuclei (e.g., protons) equalizes T_1 and $T_{1\rho}$ values among magnetically nonequivalent sites. In phase-separated polymers, the observation of identical ^{1}H T_1 relaxation rates for the two phases can be used to set an upper limit on the distance between the two phases (e.g., the lamellar thickness in a crystallite). In a similar fashion, the presence of unique ^{1}H $T_{1\rho}$ values can be used to set a lower limit. The absence of efficient ^{13}C–^{13}C spin diffusion on a time scale of several seconds is not surprising for an unlabeled polymer. The natural abundance of ^{13}C (1.1%) implies a long average internuclear separation and hence, in combination with the low magnetogyric ratio, a slow flip–flop rate.

^{31}P, with an abundance of one nucleus per repeat unit in this polymer and a moderate magnetogyric ratio, is an intermediate case with respect to spin diffusion. The short ^{31}P $T_{1\rho}$ values for the mesomorphic phase (<100 ms) define a time scale too short for appreciable magnetization transfer from one phase to the other. The ^{31}P T_1 values, on the other hand, define a time scale of seconds to tens of seconds, and the relaxation behavior observed in suitably performed T_1 measurements clearly shows that a magnetization transfer process is operative and allows its rate to be calculated. Figure 3 is a semilog plot of a typical ^{31}P T_1 measurement using the pulse sequence described by

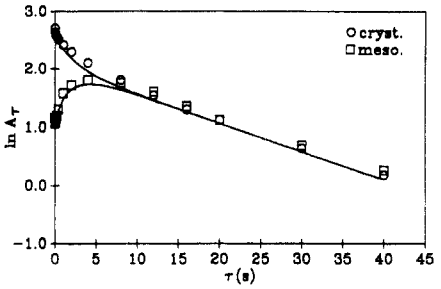

Figure 3. ^{31}P spin–lattice relaxation curves for PB3MP showing a magnetization transfer process on a time scale of ca. 3 s. The smooth curves were calculated using eqs 1 and 2 (see text).

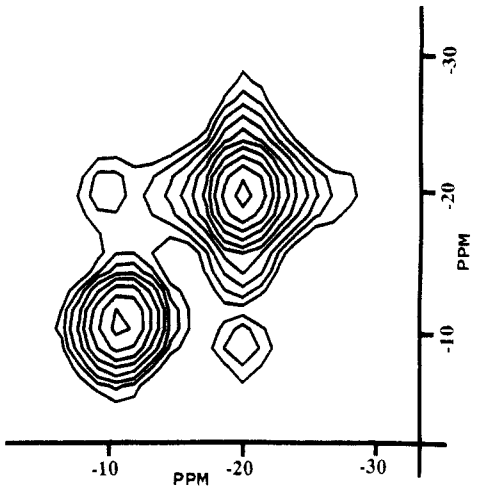

Figure 4. ^{31}P 2D exchange spectrum of PB3MP at 23 °C using a 2-s mixing time. The cross peaks connecting the diagonal resonances for the two phases confirm the existence of a magnetization transfer process.

Torchia.[26] That pulse sequence generates magnetization by cross polarization and subtracts any Bloch decay components which are uncorrelated with the cross polarization. Inspecting Figure 3, one notes that the magnetization curves converge over a time scale of ca. 3 s and then subsequently decay at a common rate. (The common intercept is coincidental.) Indeed, the magnetization of the mesomorphic peak actually increased for several seconds before beginning to decay to the equilibrium value of zero expected in the Torchia experiment. This behavior is consistent with a magnetization transfer process, either chemical exchange or spin diffusion, between the components in the respective phases. Chemical exchange would have similar effects on the relaxation curves obtained for ^{13}C and ^{1}H; since no such effects were observed, chemical exchange can be ruled out as the magnetization transfer process. The ^{31}P resonance due to the crystalline phase cross polarizes much more efficiently than that for the mesomorphic phase, creating an initial polarization gradient across the phase boundaries which spin diffusion restores on a time scale of several seconds.

T_1 values were obtained from curves like Figure 3 by fitting the slope of the magnetization plot in the longer time region (i.e., after convergence). The theoretical relaxation curves used to fit the experimental points in Figure 3 will be discussed after we present further evidence for the magnetization transfer process and an independent measurement of the spin diffusion rate.

^{31}P two-dimensional exchange spectra[24] were obtained at several mixing times. Figure 4 shows a two-dimensional spectrum obtained at a mixing time of 2 s. This spectrum clearly shows cross peaks connecting the crystalline and mesomorphic peaks of the polymer. Semiquantitative

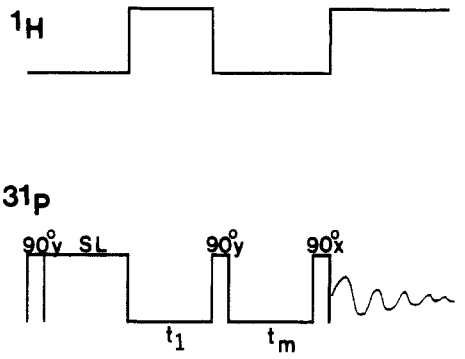

Figure 5. Pulse sequence for one-dimensional exchange experiment. t_1, evolution period; SL, spin-lock period; and t_m, mixing time.

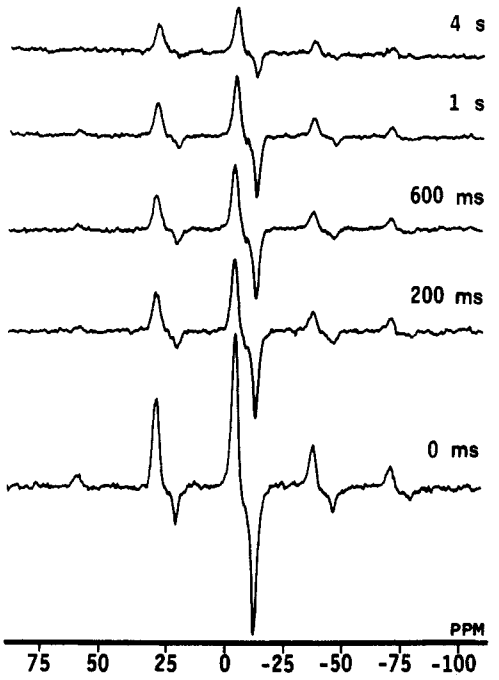

Figure 6. ^{31}P MAS one-dimensional exchange spectra of PB3MP obtained at 20 °C and various mixing times using the pulse sequence in Figure 5.

comparisons of 2D spectra obtained at various mixing times suggest a magnetization transfer rate constant of ca. 3 s. The appearance of cross peaks connecting the crystalline and mesomorphic diagonal peaks unambiguously confirms a magnetization transfer process on the time scale of a few seconds. An effort to quantify the rate constant for magnetization transfer from 2D spectra was complicated by the line shapes produced by the absolute mode transform used to process 2D exchange spectra. Maciel and co-workers have described a one-dimensional analog of the 2D experiment for determining chemical exchange rates in solids.[30] The results of that experiment are most readily interpreted if the two peaks undergoing exchange are of approximately the same intensity. In order to obtain an initial condition characterized by equal intensity for the crystalline and mesomorphic resonances, we developed the modified pulse sequence shown in Figure 5. Coherence is created by a 90° pulse and is then held in a spin-lock for a time sufficiently long (typically several milliseconds) to equalize the magnetization through the short $T_{1\rho}$ for the mesomorphic phase (Table I). ^{31}P magnetization evolves under isotropic chemical shift interactions during the interval t_1, which corresponds to the time required to achieve a 180° phase difference between the two resonances. (The spinning speed is adjusted for this experiment such that t_1 also corresponds to an integer multiple

Table IV
^{31}P–^{31}P Spin Diffusion Rates between the Two Phases of PB3MP

	rate, k (s^{-1})	
temp (°C)	without ^1H decoupling	with ^1H decoupling
25	0.35	0.30
40	0.30	0.24
60	0.31	0.23

of the rotor period.) The second 90° pulse creates a condition in which the magnetization from one peak is along $+z$ while that from the other is along $-z$. Magnetization transfer is allowed to occur during a variable mixing time (t_m) prior to detection. The results of a representative experiment are shown in Figure 6. The decrease in signal intensity as a function of time was fit to an exponential model to yield the characteristic exchange time constant $\tau = k_{ex}^{-1}$. This experiment was performed at three different temperatures (Table IV). The observation that the magnetization transfer rate (ca. 0.30 s^{-1}) is temperature independent is consistent with the fact that spin diffusion is not a thermally activated process and further rules out chemical exchange as the magnetization transfer mechanism.

The theoretical curves used to fit the experimental data points in Figure 3 were calculated from the following coupled differential equations:[31]

$$\frac{dM_z(\text{cryst})}{dt} = \frac{M_z^0(\text{cryst}) - M_z(\text{cryst})}{T_1(\text{cryst})} - k_{ex}M_z(\text{cryst}) + k_{ex}M_z(\text{meso}) \quad (1)$$

$$\frac{dM_z(\text{meso})}{dt} = \frac{M_z^0(\text{meso}) - M_z(\text{meso})}{T_1(\text{meso})} - k_{ex}M_z(\text{meso}) + k_{ex}M_z(\text{cryst}) \quad (2)$$

The M_z^0 terms designate the equilibrium magnetization of the respective phases. These equations were solved numerically using the Runga–Kutta method[32] and initial conditions obtained from measurements of cross polarization efficiencies for the two phases. A number of simulations were performed using different T_1 values and different values of k_{ex}. The simulation in Figure 3 was carried out using the experimentally obtained values of k_{ex} (0.30 s^{-1}, Table IV) and $T_1(\text{meso}) = T_1(\text{cryst}) = 20$ s (Table III). On examining Figure 3, one notes an excellent agreement between theory and experiment. We conclude that the seemingly anomalous behavior of the ^{31}P T_1 data for this polymer is fully accounted for by a spin diffusion process which transfers magnetization between the two phases with a rate constant of 0.30 s^{-1}. As we will show presently, this value can be used to calculate a characteristic dimension (domain size) for the crystalline phase. First, however, we wish to make several comments on the likely mechanism of the spin diffusion process.

The rate at which spin diffusion occurs is related to the zero-quantum transition probability as determined via first-order perturbation theory. This transition rate is maximized for spectral density at zero frequency, i.e. for overlapping resonances. Strictly speaking, the zero-quantum transition rate is proportional to the density of energy conserving spin–spin flip–flops, that is the probability that single-quantum transitions occur at the same frequency. For single-quantum transitions that occur at different frequencies, the energy imbalance must be compensated for via one or more of several possible contributions from the lattice. This process is entirely analogous to the zero-quantum transition that occurs in heteronuclear NOE's in that the required energy comes from the lattice. Furthermore, cross polarization in solids involves the same type of argument in that the maximum transfer rate occurs when the two nuclei are given the same precessional frequency in the rotating frame.

In the ^{31}P MAS NMR spectrum of PB3MP, the peaks corresponding to the crystalline and mesomorphic phases are separated by 1.02 kHz. Therefore, the zero-quantum transition is not secular. Spin diffusion between nuclei with different resonance frequencies has been observed.[33] In order for spin diffusion to occur in this case, there must exist some mechanism by which the energy difference is accounted for. In previous contributions, several workers have found that the most common mechanism for providing the energy needed to compensate for the imbalance is through heteronuclear dipolar coupling to a large reservoir of proton spins.[33-36] Rapid spin diffusion occurs due to the large homonuclear dipolar interactions between nearby protons. In the one-dimensional exchange experiment, Figure 5, proton decoupling is absent during the mixing period. As such, the ^{31}P–^1H dipolar interaction leads to broad line widths and significant spectral overlap of the two peaks. The rate at which spin diffusion occurs is a function of the degree of overlap of the resonances.[34] If proton decoupling is applied during the mixing period, the spectral overlap will decrease. As a result, the diffusion rate should also decrease. If spin diffusion occurs via the proton dipolar reservoir, removal of the ^{31}P–^1H interactions should change the spin diffusion process rate constant. When decoupling was applied during the mixing period, the spin diffusion rates at the three temperatures studied decreased approximately 20% (Table IV). However, as is evident in Figure 1, significant spectral overlap remains at temperatures ≤60 °C. Therefore, the proton reservoir most likely provides the required energy for spin diffusion. However, it is also possible that modulation of the dipolar interactions by molecular motion contributes to satisfying the energy imbalance.[34]

We now return to the physical significance of our experimentally determined ^{31}P spin diffusion rate in PB3MP. VanderHart has proposed[15] that the distance, x, over which ^1H spin diffusion occurs during a time, t, can be modeled as

$$x^2 = {}^4/_3Dt \quad (3)$$

The diffusion constant D was originally calculated to be 6.2×10^{-12} cm^2 s^{-1} for protons in polyethylene by Douglass and Jones.[37] VanderHart proposed that this value could be used in his studies of ^1H spin diffusion in poly(ethylene terephthalate) following appropriate correction for the relative densities of protons in those materials.[15] In a similar fashion, we estimated a ^1H diffusion constant for PB3MP of 4.3×10^{-12} cm^2 s^{-1}. In order to estimate a ^{31}P diffusion constant, it was necessary to scale the polyethylene spin diffusion constant by both a spin density correction and a magnetogyric ratio (γ) correction

$$D_{\text{PB3MP}}^{\ ^{31}P} = D_{\text{PE}}^{\ ^1H} \frac{[^{31}P]_{\text{PB3MP}}^{1/3}\gamma_{^{31}P}^4}{[^1H]_{\text{PE}}^{1/3}\gamma_{^1H}^4} \quad (4)$$

from which we obtained a value of 4.8×10^{-14} cm^2 s^{-1}. The observation that the ^1H T_1 values are identical in the two phases while the ^1H $T_{1\rho}$ values are unique allows upper and lower limits on the characteristic domain sizes to be established by equating T_1 and $T_{1\rho}$, respectively, to t in eq 3. This procedure allows us to estimate a lower limit of 3.1 nm and an upper limit of 37 nm. Since the ^{31}P

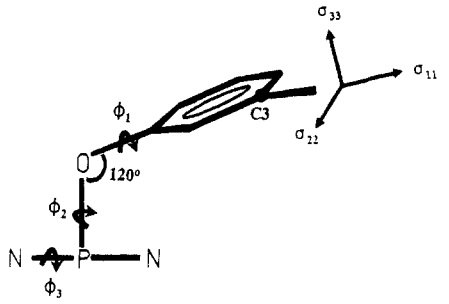

Figure 7. Schematic diagram of the model used to interpret slow-speed ^{13}C MAS spectra of PB3MP in terms of molecular motion in the mesomorphic phase. ϕ_1, ϕ_2, and ϕ_3 designate the three continuous diffusional processes used in simulations. The assumed orientation of the shielding tensor of C3 is indicated (see text).

spin-diffusion rate is accurately known, a more exact calculation is possible. Using our estimate of the ^{31}P spin-diffusion constant, we arrive at a characteristic size of 4.5 nm, a value consistent with the limits established by the ^1H data. Our physical interpretation of the 4.5-nm value is somewhat speculative, but it is consistent with Vander-Hart's treatment.[38] We interpret the characteristic size as $^1/_2$ the lamellar thickness of the crystallites. Our lamellar thickness of 9 nm is consistent with the range expected for organic polymers.[39] The observation that the ^{31}P spin diffusion rate is temperature independent implies that the average thickness does not change over the course of the phase transition.

We now consider the relationship between the mesomorphic transition and molecular dynamics. A detailed picture of molecular motion in solids can often be obtained by comparing the calculated effects of physically reasonable models of motion on one or more line broadening interactions and comparing simulations and experiments. ^2H line shape analysis is a *spectroscopically* convenient way of determining the types and amplitudes of motion at a particular nuclear site, but the need to prepare several selectively labeled polymers makes this approach less attractive. Our approach to the study of molecular dynamics in PB3MP has been to make use of the chemical shift interaction. Herzfeld and Berger have shown how the principal components of the chemical shift tensor can be calculated from the amplitudes of an isotropic peak and two or more orders of spinning sidebands.[40] It is possible, therefore, to measure motionally-averaged principal components for multiple nuclear sites from slow-speed MAS spectra—without the requirement of multiple selective enrichments. Using this procedure we first determined that there is negligible motion of the 3-methylphenoxy side group in the crystalline phase of PB3MP. This was done by comparing calculated ^{13}C principal component data obtained selectively from the crystalline phase for C3 (σ_{11} = 230, σ_{22} = 162, and σ_{33} = 31 ppm) by cross polarization with analogous measurements obtained for C3 in the model compound *m*-cresol (σ_{11} = 229, σ_{22} = 165, and σ_{33} = 29 ppm) at a temperature of −70 °C. In contrast to the negligible motion found in the crystalline phase, side groups in the mesomorphic phase must be undergoing large amplitude motions as suggested by the near absence of sidebands in Figure 2b. In order to characterize what motions the side groups undergo in the mesomorphic phase of PB3MP, we made use of the model shown in Figure 7. The shielding tensor orientation shown in Figure 7 is that reported for C1 in *p*-xylene.[41] A survey of the literature[42] suggests that this orientation is typical for alkyl-substituted aromatic carbons. The principal components of the tensor used for simulations were

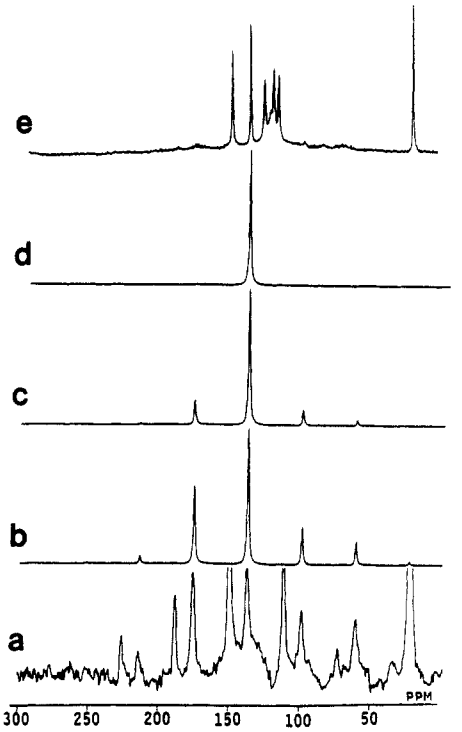

Figure 8. Experimental and simulated ^{13}C MAS spectra probing motion in the mesomorphic phase of PB3MP: (a) cross polarization spectrum with interrupted decoupling spectrum showing C3, C1, and CH_3 in the crystalline phase; (b) simulated spectrum of C3 showing the effect of motion ϕ_1; (c) simulated spectrum of C3 showing the effect of ϕ_1 and ϕ_2; (d) simulated spectrum of C3 showing the effect of ϕ_1, ϕ_2, and ϕ_3; (e) Bloch decay spectrum of PB3MP showing all signals from the mesomorphic phase. The cross polarization and Bloch decay spectra were obtained at −50 and 23 °C, respectively. All spectra are at a spinning speed of 2900 Hz.

obtained by a procedure analogous to the method of Waugh and co-workers.[43]

Figure 8a shows a ^{13}C CP/MAS spectrum of PB3MP obtained with 50 μs of interrupted decoupling to suppress signals due to the protonated aromatic carbons. The region of this spectrum between 50 and 250 ppm has features exclusively due to the isotropic peaks and first- and second-order spinning sidebands of C1 and C3. Figure 8e shows a Bloch decay spectrum of the mesomorphic phase (with the crystalline phase completely saturated) at the same spinning speed as in Figure 8a, 2900 Hz. Figures 8b–d show simulated spectra of C3 incorporating the progressive effect of the three physically reasonable motions depicted in Figure 7. Figure 8b shows that a modest amount of averaging is obtained by permitting the rapid continuous diffusional process ϕ_1. The combination of ϕ_1 and ϕ_2 leads to significant averaging of the chemical shift anisotropy of C3 (Figure 8c), but not nearly enough to account for the near-total loss of sideband intensity for C3 in the mesomorphic phase. ϕ_1 and ϕ_2 are the only physically reasonable large-amplitude processes that can take place without torsional motion of one repeat unit relative to its neighbors or motion of the nuclear coordinates of the P and N atoms. The simulation in Figure 8d also includes the effects of continuous torsional motion (ϕ_3, Figure 7). Comparing parts d and e of Figure 8, one notes that the necessary amount of averaging can be obtained by the combination of ϕ_1, ϕ_2, and ϕ_3. On the basis of Figure 8 alone, we cannot prove that the sole motion of the polymer chain is torsional, but these results do show that local motions of the aryl groups alone are insufficient to account for the motional averaging of the ^{13}C shift anisotropy in the mesomorphic phase.

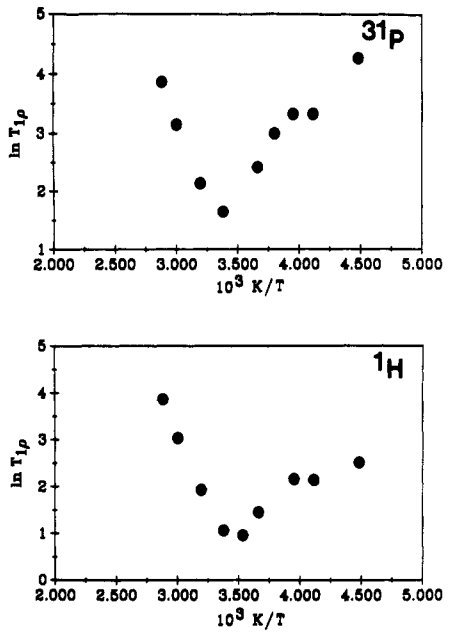

Figure 9. Arrhenius plots of the temperature dependence of the ^{31}P $T_{1\rho}$ and ^{1}H $T_{1\rho}$ values for the mesomorphic phase of PB3MP.

The temperature-dependent $T_{1\rho}$ measurements for the mesomorphic phase in Table I provide information about the frequency of molecular motion in this polymer. Figure 9 shows Arrhenius plots of these data. Examining that figure, one notes a strong qualitative similarity between the ^{1}H and ^{31}P relaxation behavior, suggesting that these are sensitive to the same molecular dynamics. Both plots show narrow plateaus in the vicinity of T_g (−25 °C) and $T_{1\rho}$ minima in the vicinity of 23 to −10 °C. Since both measurements were performed with spin-lock fields (γB_1) of 58 kHz, the motion responsible for $T_{1\rho}$ relaxation is characterized by that frequency in the vicinity of the $T_{1\rho}$ minima. From the slopes of the Arrhenius plots in the extreme narrowing limits, activation energies of 11.2 and 9.0 kcal/mol were calculated for the ^{1}H and ^{31}P data, respectively. Using molecular mechanics calculations, Allcock[44] has shown that the barrier height for torsional motion (in several poly(alkoxyphosphazenes) and poly[bis(phenoxy)phosphazene]) increases with the size of the substituent. For poly[bis(phenoxy)phosphazene], Allcock reports a value of 5.2 kcal/mol. Since PB3MP has an even larger substituent, it is not unreasonable to assume that the activation energies (ca. 10 kcal/mol) obtained from our Arrhenius plots are due to torsional motion of the polymer chain. Pre-exponential factors could not be calculated with a high degree of confidence because of uncertainties in the $T_{1\rho}$ measurements, but the values were estimated using standard relaxation theory to be on the order of 1×10^{-13} s for the two plots in Figure 9.

Summary

This report has described the use of a number of NMR methods to characterize the morphology of a representative semicrystalline polyphosphazene. One novel feature of this contribution is the detailed investigation of ^{31}P spin diffusion. This phenomenon occurs on a time scale such that it shows up as an apparent anomaly in suitable performed ^{31}P T_1 measurements. *It is clear that the spin diffusion regime between the more familiar cases of ^{1}H and ^{13}C at natural abundance deserves additional attention.*

Detailed measurements of relaxation rates and motionally-averaged chemical shift anisotropies in combination with the ^{31}P spin diffusion rate measurement have been interpreted to give the following picture of the morphology of PB3MP. The crystallites in this polymer have lamellae that are ca. 9 nm thick. Large-amplitude molecular motions (except for the trivial case of methyl rotation) are not possible in the crystalline phase. Large-amplitude motions in the mesomorphic phase include unrestricted rotation of the side group and torsional motion along the main chain.

Acknowledgment. This work was supported by the Office of Naval Research. The NMR spectrometer was purchased with funds provided by a Department of Defense instrument grant. S.A.T. is an NSF Chemistry Division Fellow and a Texas A&M University Minority Merit Fellow. J.L.W. is a Dow Chemical Graduate Fellow. N.C.E. is a Robert A. Welch Foundation Fellow. We gratefully acknowledge M. Peters, J. Munch, R. Andrejak, and J. Feldman of W. R. Grace for their assistance in obtaining polymer characterization data.

References and Notes

(1) Earl, W. L.; VanderHart, D. L. *Macromolecules* **1979**, *12*, 762.
(2) Fyfe, C. A.; Lyerla, J. R.; Volksen, W.; Yannoni, C. S. *Macromolecules* **1979**, *12*, 757.
(3) Belfiore, L. A.; Schilling, F. C.; Tonelli, A. E.; Lovinger, A. J.; Bovey, F. A. *Macromolecules* **1984**, *17*, 2561.
(4) Bloembergen, N.; Purcell, E. M.; Pound, R. V. *Phys. Rev.* **1948**, *73*, 679.
(5) Jelinski, L. W.; Schilling, F. C.; Bovey, F. A. *Macromolecules* **1981**, *14*, 581.
(6) Jelinski, L. W.; Dumais, J. J.; Engel, A. K. *Macromolecules* **1983**, *16*, 403.
(7) Sefcik, M. D.; Schaefer, J.; Stejskal, E. O.; McKay, R. A. *Macromolecules* **1980**, *13*, 1132.
(8) Schaefer, J.; Stejskal, E. O.; Perchak, D.; Skolnick, J.; Yaris, R. *Macromolecles* **1985**, *18*, 306.
(9) Schaefer, J.; Sefcik, M. D.; Stejskal, E. O.; McKay, R. A.; Dixon, W. T.; Cais, R. E. *Macromolecules* **1984**, *17*, 1107.
(10) Miura, H.; English, A. D. *Macromolecules* **1988**, *21*, 1543.
(11) Henrichs, P. M.; Linder, M.; Hewitt, J. M.; Massa, D.; Isaacson, H. V. *Macromolecules* **1984**, *17*, 2412.
(12) Henrichs, P. M.; Luss, H. R. *Macromolecules* **1988**, *21*, 860.
(13) Bloembergen, N. *Physica* **1949**, *15*, 386.
(14) Abragam, A. *The Principles of Nuclear Magnetism*; Oxford University: Oxford, 1961; p 138.
(15) Havens, J. R.; VanderHart, D. L. *Macromolecules* **1985**, *18*, 1663.
(16) VanderHart, D. L. *J. Magn. Reson.* **1987**, *72*, 13.
(17) Tanaka, H.; Gomez, M. A.; Tonelli, A. E.; Chichester-Hicks, S. V.; Haddon, R. C. *Macromolecules* **1989**, *22*, 1031.
(18) Komoroski, R. A., Ed. *High Resolution NMR Spectroscopy of Synthetic Polymers in Bulk*; VCH Publishers: Deerfield Beach, FL, 1986.
(19) Crosby, R. C.; Haw, J. F. *Macromolecules* **1987**, *20*, 2324.
(20) Crosby, R. C.; Haw, J. F.; Lewis, D. L. *Anal. Chem.* **1988**, *60*, 2697.
(21) Alexander, M. N.; Desper, C. R.; Sagalyn, P. L.; Schneider, N. S. *Macromolecules* **1977**, *10*, 721.
(22) Schneider, N. S; Desper, C. R.; Singler, R. E.; Alexander, M. N.; Sagalyn, P. L. *Organometallic Polymers*; Carraher, C. E., Jr., Sheats, J. R., Pitman, C. U., Jr., Eds.; Academic Press: New York, 1978.
(23) Young, S. G.; Magill, J. H. *Macromolecules* **1989**, *22*, 2551.
(24) Szeverenyi, N. M.; Sullivan, M. J.; Maciel, G. E. *J. Magn. Reson.* **1982**, *47*, 462.
(25) Jeener, J.; Meier, B. H.; Bachmann, P.; Ernst, R. R. *J. Chem. Phys.* **1979**, *71*, 4546.
(26) Torchia, D. A. *J. Magn. Reson.* **1978**, *30*, 613.
(27) Sullivan, M. J.; Maciel, G. E. *Anal. Chem.* **1982**, *54*, 1615.
(28) Crosby, R. C. Ph.D. Dissertation, Texas A&M University, 1988.
(29) Schaefer, J.; Stejskal, E. O.; Steger, T. R.; Sefcik, M. D.; McKay, R. A. *Macromolecules* **1980**, *13*, 1121.
(30) Szeverenyi, N. M.; Bax, A.; Maciel, G. E. *J. Am. Chem. Soc.* **1983**, *105*, 2579.
(31) McConnell, H. M. *J. Chem. Phys.* **1958**, *28*, 430.
(32) Zill, D. G. *A First Course in Differential Equations with Applications*; PWS Publishers: Boston, 1986; p 454.
(33) Suter, D.; Ernst, R. R. *Phys. Rev. B* **1985**, *32*, 5608.

(34) Henrichs, P. M.; Linder, M.; Hewitt, J. M. *J. Chem. Phys.* **1986**, *85*, 7077.
(35) Kubo, A.; McDowell, C. A. *J. Chem. Soc., Faraday Trans. 1* **1988**, *84*, 3713.
(36) Limbach, H.; Wehrle, B.; Schlabach, M.; Kendrick, R.; Yannoni, C. S. *J. Magn. Reson.* **1988**, *77*, 84.
(37) Douglass, D. C.; Jones, G. P. *J. Chem. Phys.* **1966**, *45*, 956.
(38) VanderHart, D. L. *Macromol. Chem., Macromol. Symp.* **1990**, *38*, 125.
(39) Bassett, D. C. *Principles of Polymer Morphology*; Cambridge University: Cambridge, 1981; p 46.
(40) Herzfeld, J.; Berger, A. E. *J. Chem. Phys.* **1980**, *73*, 6021.
(41) van Dongen Torman, J.; Veeman, W. S. *J. Chem. Phys.* **1978**, *68*, 3233.
(42) Veeman, W. S. *Progr. NMR Spectrosc.* **1984**, *16*, 193.
(43) Mehring, M.; Griffin, R. G.; Waugh, J. S. *J. Chem. Phys.* **1971**, *55*, 746.
(44) Allen, R. W.; Allcock, H. A. *Macromolecules* **1976**, *9*, 956.